ELSEVIER

Catalysis Today 79–80 (2003) 105–111

CATALYSIS TODAY

www.elsevier.com/locate/cattod

# A new concept reactor for hydrocarbon hydrogenation in the reactive evaporation mode

N.A. Kuzin, A.V. Kulikov, A.B. Shigarov*, V.A. Kirillov

*Boreskov Institute of Catalysis, Prosp. Akad. Lavrentieva 5, 630090 Novosibirsk, Russia*

## Abstract

A new gas–liquid–solid reactor is presented whose concept is based on the coupling of liquid imbibition, evaporation, and an exothermic gas-phase reaction within a non-permselective catalytic porous membrane. Because of enhanced thermal conductivity of the sintered metal catalyst support and liquid flow re-circulation, it is possible to eliminate hot spots and runaways and to maintain high productivity of the reactor. When vapor conversion in the membrane is high, the problem of separation of the product from the gas phase reduces to common condensation. The preliminary experiments on the α-methylstyrene (AMS) hydrogenation on the 10% (0.9% Pd/$\gamma$-$Al_2O_3$) + 90% (80% Ni, 20% Al) membrane sintered on the tube wall are very promising, however, further investigations are required.

*Keywords:* Hydrocarbon hydrogenation; Novel multiphase reactor; Non-permselective membrane; Sintered metal catalyst support; Imbibition; Evaporation

## 1. Introduction

The essential part of heterogeneous catalytic multiphase reactions in the chemical and petrochemical industries involves hydrogenation of hydrocarbons. Such catalytic reactions are characterized by high intrinsic kinetic rate and are mildly exothermic. The value of heat effect of the completely hydrogenated undiluted liquid phase is usually several times higher than that required for its vaporization. Solubility of hydrogen in liquid hydrocarbons is weak and the liquid-phase transport is very slow. So, various aspects of mass and heat transport limitations play, as a rule, an important role in industrial reactors. The disadvantages of conventional hydrogenation reactors are well known. For the slurry reactors, there are problems with separation of a catalyst and its limited concentration in the liquid phase. The bubble-column reactors with a fixed catalyst bed suffer from both poor mass transfer and extremely low catalyst efficiency. The trickle-bed reactors are also characterized by liquid muldistribution, hot spots and runaway phenomena. That is why the trickle-bed reactors require: dilution of liquid reactants, high pressure operation and multi-stage configurations. So, all conventional liquid-phase hydrocarbon hydrogenation reactors provide thermal safety at the expense of their low productivity (i.e. large reactor dimensions).

The above factors explain the reason of high research activity of different groups in developing of new multiphase reactors or updating of the conventional reactors. A new hydrogenation technology was presented elsewhere [1], in which a fixed-bed reactor is used with a liquid-phase flow (without the gas phase). Though this technology requires an additional unit for saturation of liquid with hydrogen, it helps to eliminate hot spots and runaways. Vaarkamp et al. [2]

---

* Corresponding author.
*E-mail address:* shigarov@catalysis.nsk.su (A.B. Shigarov).

0920-5861/03/$ – see front matter © 2003 Elsevier Science B.V. All rights reserved.
doi:10.1016/S0920-5861(03)00016-6

have experimentally tested this idea in the monolithic reactor. Another approach employs a structured monolith catalyst and a two-phase flow (slugging regime). This approach was first described in the early work of Hatziantoniou and Andersson [3] and was developed in recent publications of Andersson et al. [4] and Nijhuis et al. [5].

The application of non-permselective inorganic catalytic membrane reactors is an alternative approach. Gas and liquid flows contact with the opposite sides of the membrane. The porous membrane serves as a diffusion barrier and a catalyst at a time. de Vos et al. [6] used a cross-flow reactor supplied with thin ceramic plates acting as a catalyst support for the liquid-phase hydrogenation of nitrobenzoic acid. Cini and Harold [7] used a tubular membrane reactor with a macro porous wall and a micro porous active film to provide hydrogenation of AMS at the normal pressure. Similar reactors were used by Peureux et al. [8] for the nitrobenzene hydrogenation.

According to the mathematical modeling of half-wetted and partially liquid filled catalyst slab [9], a sharp increase in the apparent reaction rate may occur, if evaporation and the vapor-phase reaction take place within the slab. The experiments [10] on cyclohexene hydrogenation occurring on a single partially wetted catalyst pellet provide support for the effect of rate enhancement (to 50 times) at normal pressure. The experimental investigation of this effect on different catalytic pellets during AMS hydrogenation was reported in detail elsewhere [11]. The mathematical models describing the ignition/extinction phenomena observed in [11] have been developed by Shigarov et al. [12]. The goal of this research was to use the effect of rate enhancement (based on the coupling of evaporation and the gas-phase reaction within an “ignited” catalyst) for developing a novel concept reactor for liquid hydrocarbon hydrogenation. This work presents the principle, the first experimental realization and preliminary experimental tests of such a reactor.

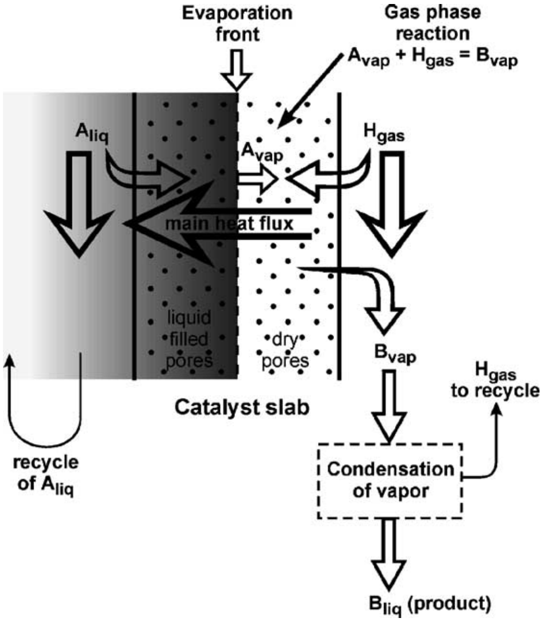

Fig. 1. Principle of the novel multiphase reactor for hydrogenation of hydrocarbons.

## 2. Experimental

### 2.1. Basic principle of the novel reactor design

We consider a heterogeneously catalyzed exothermic reaction, $A + H_{gas} = B$, assuming that the value of reaction heat exceeds that required for the complete liquid-phase evaporation. The following idealized scheme of the reactor (Fig. 1) is suggested. One side of the catalyst slab contacts with a liquid reactant flow, the opposite side is in contact with a gaseous reactant flow. The liquid reactant is imbibed inside the porous slab due to capillary forces. The evaporation front is situated inside the slab. Above the front, there is a dry pore zone where the gas-phase reaction occurs. When reactant $A$ is completely converted in the slab, only vapor $B$ (product) is removed into the gas flow. The main part of heat, produced by the reaction (accounting evaporation) is removed into the liquid flow. Therefore, a rather high conductivity of the catalyst support and high liquid velocity are required for enhancing the liquid–solid heat transfer. It is evident that in order to maintain reasonable temperature gradients (since an adiabatic temperature rise is usually too high), a liquid reactant re-circulation accompanied by external cooling is required.

### 2.2. Reactor and catalyst

The reactor (Fig. 2) is designed as a perforated steel tube with 22 openings for distribution of the AMS

Table 1
Parameters of the reactor

| Length of tube (mm) | Outer diameter of tube (mm) | Inner diameter of tube (mm) | Thickness of sintered catalyst layer (mm) | Reactor diameter (mm) | Number of openings | Liquid AMS flow rate (mg/s) |
|---|---|---|---|---|---|---|
| 110 | 8 | 6 | 7.5 | 23 | 22 | 430 |

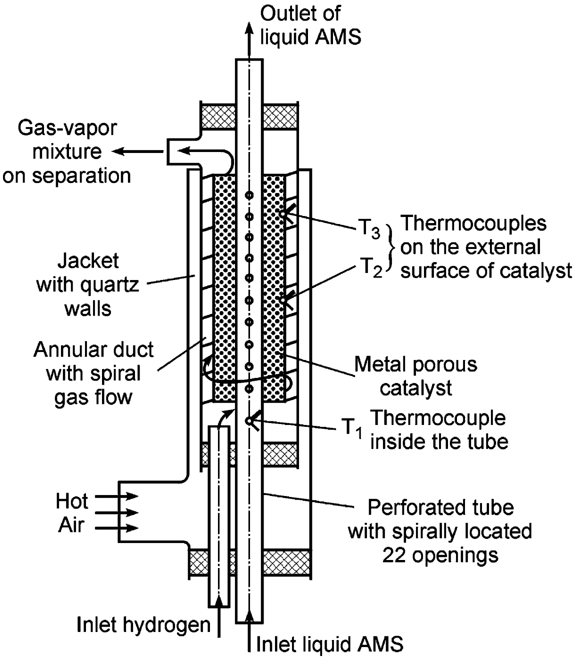

Fig. 2. Tubular reactor for AMS hydrogenation.

liquid inside the reactor. The reactor parameters are given in Table 1. The openings are directed in spiral along the tube. The external surface of this tube is sintered with the composite porous catalyst. The detailed procedure of the catalyst preparation is based on the methods of powder metallurgy. The catalyst characteristics are given in Table 2. To compensate heat losses, the reactor is placed into a hot air jacket. In order to enhance the solid–gas mass transfer, the spiral channels are incorporated into an annular duct. The reactor is supplied with three thermocouples for measuring inlet liquid temperature $T_1$ and external catalyst surface temperature at the middle $T_2$ and at the outlet $T_3$ of the reactor.

### 2.3. Experimental measurements and procedures

A start-up procedure of the reactor is as follows. An air preheating unit begins to feed air and hydrogen. Then AMS is fed through the liquid preheating unit. As the temperature transition period is completed, the steady state data are taken.

The apparent rate of AMS evaporation is defined as the rate of vapor condensation in the outlet condenser unit. The condensed mixture samples were analyzed chromatographically. As found, cumene is the only product of AMS hydrogenation. Thus, the AMS conversion was merely determined as the fraction of cumene in the mixture of these two vapors. The apparent reaction rate was calculated as the product of AMS evaporation rate and AMS conversion. The as-defined (and accepted in this work) “reaction rate” is not an intrinsic rate, this value indicates productivity of the reactor volume.

## 3. Results and discussion

Visual observations of the external catalyst surface permit one to detect wet zones that distinguished by a dark color. The preliminary runs showed that if a wet

Table 2
Parameters of the sintered catalyst layer

| Sintered mixture powder content (mass%) | | | Pore surface ($m^2/g$)[a] | Pore volume ($cm^3/g$)[b] | Main pore diameter (μm)[b] |
|---|---|---|---|---|---|
| Ni | Al | 0.9% Pd/γ-$Al_2O_3$ | | | |
| 72 | 18 | 10 | 4 | 0.315 | 10–30 |

[a] BET argon desorption method data.
[b] Mercury porosimetry data.

Table 3
Experimental results

| Diameter of openings (mm) | Hydrogen flow rate ($cm^3/s$) | $T_1$ (°C) | $T_2$ (°C) | $T_3$ (°C) | Vapor condensation rate (mg/s) | AMS conversion (%) | Reaction rate ($mol/m^3$ s)[a] |
|---|---|---|---|---|---|---|---|
| 0.7 | 43.5 | 100 | 128 | 128 | 7.7 | 98.9 | 1.40 |
| | 55 | | 125 | 132 | 9.6 | 99.8 | 1.77 |
| | 100 | | 124 | 130 | 9.0 | 98.8 | 1.62 |
| | 43.5 | 110 | 138 | 138 | 7.7 | 99.5 | 1.40 |
| | 55 | | 134 | 134 | 7.4 | 99.8 | 1.36 |
| | 100 | | 131 | 131 | 6.9 | 99.92 | 1.28 |
| | 43.5 | 121 | 147 | 147 | 6.9 | 99.85 | 1.25 |
| | 55 | | 140 | 140 | 5.5 | 99.8 | 1.00 |
| | 100 | | 139 | 139 | 5.7 | 99.8 | 1.04 |
| | 43.5 | 131 | 154 | 153 | 5.9 | 99.8 | 1.08 |
| | 55 | | 153 | 152 | 5.3 | 99.85 | 0.96 |
| | 100 | | 150 | 150 | 4.5 | 99.8 | 0.81 |
| 1.0 | 43.5 | 131 | 271 | 264 | 21.8 | 97.2 | 3.83 |
| | 55 | | 247 | 246 | 20.6 | 98.8 | 3.76 |
| | 100 | | 233 | 233 | 17.4 | 94.6 | 3.02 |
| | 43.5 | 150 | 263 | 256 | 20.5 | 99.2 | 3.68 |
| | 55 | | 257 | 250 | 17.9 | 99.3 | 3.24 |
| | 100 | | 250 | 244 | 15.1 | 99 | 2.73 |
| | 43.5 | 163 | 265 | 257 | 22.2 | 98.5 | 3.83 |
| | 55 | | 253 | 248 | 17.6 | 98.8 | 3.17 |
| 1.4 | 43.5 | 131 | 151 | 124 | 127.6 | 34 | 7.96 |
| | 55 | | 195 | 187 | 74.8 | 57 | 7.81 |
| | 100 | | 161 | 151 | 63.0 | 55 | 6.34 |

[a] Apparent reaction rate (productivity) per unit volume of tube, including externally sintered catalyst layer.

spot appears, then the whole external surface will be gradually wetted and the AMS conversion reduces to zero. This observation suggests that the reactor operation is supported only by the vapor-phase reaction. Indeed, hydrogen solubility in liquid AMS at normal pressure is not high and one can assume that an impact of the liquid-phase hydrogenation rate is negligible compared to that of the rate of AMS vaporization from the wet external surface to hydrogen flow. The below experimental data belong to the completely dry external catalyst surface. The experimental conditions and results are summarized in Table 3. The conversion of AMS is >94%, excepting the case of a tube with the maximum opening diameter of 1.4 mm. The highest hydrogenation rate (6.34–7.96 $mol/m^3$ s) is achieved for this maximum diameter. When the opening diameter is minimal (0.7 mm), temperatures $T_2$ and $T_3$ of the external catalyst surface are lower than the boiling point of AMS (165.4 °C). As the inlet temperature is increased from 100 to 131 °C and the hydrogen flow rate ranges from 43.5 to 100 $cm^3/s$, the difference between the external surface and inlet liquid temperatures ($T_{in} = T_1$) does not change significantly (15–30 °C). These observations suggest a slight change in the reaction rate (0.81–1.4 $mol/m^3$ s). When the opening diameter is 1 mm, the temperature difference rises to 90–140 °C, and the reaction rate approaches 2.73–3.83 $mol/m^3$ s. The external surface temperature (233–271 °C) significantly exceeds the boiling point.

Fig. 3 shows the apparent evaporation and reaction rates and AMS conversion as the functions of the openings area fraction *f*. The continuous curves of rates of evaporation $W_e(f)$ and conversion $X(f)$ represent quadratic three-point interpolations of experimental data. The curve of the reaction rate is defined by multiplication $W_r(f) = W_e(f)X(f)$. When the diameter of openings (or its fraction *f*) is increased, the

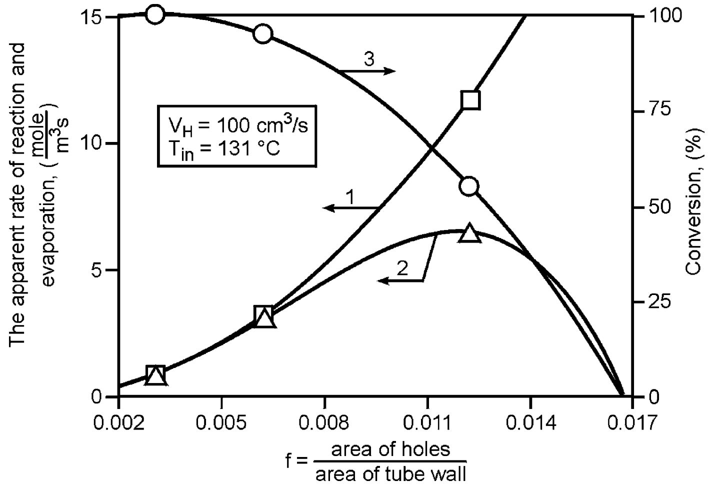

Fig. 3. Area fraction f of tube openings vs. apparent evaporation rate (1); apparent reaction rate (2); and AMS conversion (3).

rates of evaporation and reaction increase at a time until the conversion degree maintains high. In this case, productivity of the reactor depends on the evaporation rate. The latter is controlled by a fraction (or diameter) of the wall openings. When AMS conversion significantly decays, the reaction rate goes through its maximum and begins to decrease. One may suppose that productivity of the reactor under these conditions is limited by thickness of the dry catalyst layer, which does not provide full AMS conversion.

Fig. 4 shows that the rate of hydrogen flow slightly hinders the reaction rate. This observation can be associated with a cooling of the catalyst, because a hydrogen flow is not preheated before entering the reactor and a liquid flow is heated during the experiment. This cooling is confirmed by a decrease in $T_2$ and $T_3$ as the

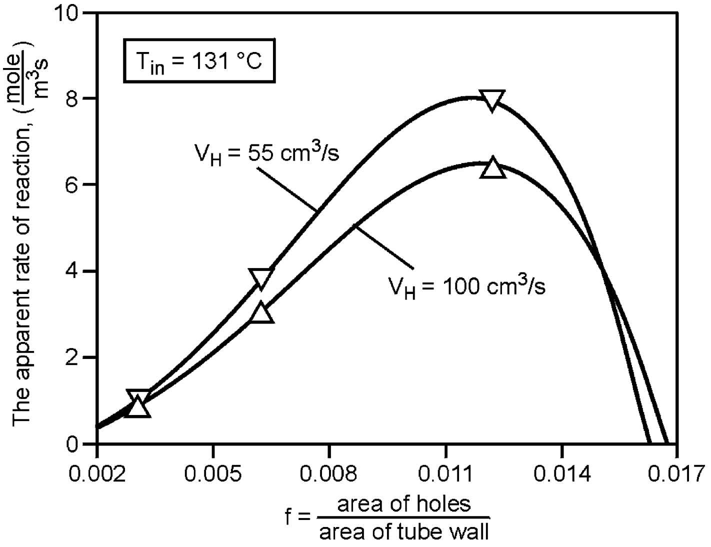

Fig. 4. Area fraction f of tube openings vs. apparent reaction rate at varied hydrogen flow rates.

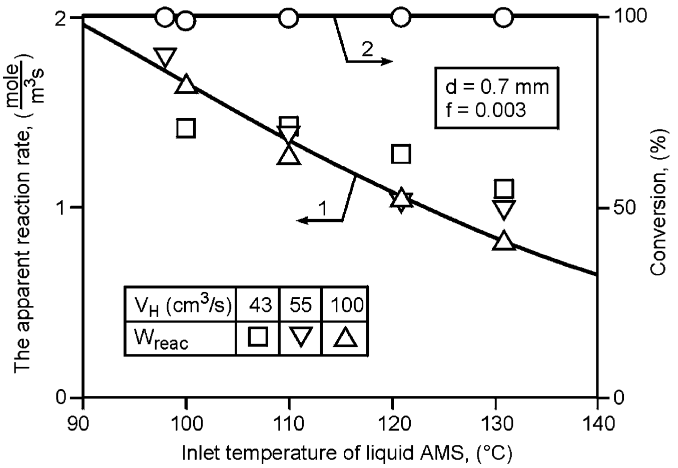

Fig. 5. Inlet liquid temperature $T_{in} = T_1$ vs. apparent reaction rate (1); and AMS conversion (2).

hydrogen flow rate increases (Table 3). The influence of temperature of inlet liquid AMS on the apparent reaction rate and AMS conversion is shown in Fig. 5. Since at the conditions of these runs, conversion is high, the apparent rate of vapor-phase hydrogenation reflects the rate of evaporation. From the above experiments, one can draw the conclusion that the apparent reaction rate is controlled by mass transfer in the dry pore zone.

In Fig. 6 the apparent rate of AMS hydrogenation (productivity per unit volume) is compared for different laboratory reactors as a slurry reactor [13], a trickle-bed reactor [5], a monolith reactor [5], a reactor with a tubular membrane [7] and our new reactor. The productivity of the novel reactor (at normal pressure) is comparable with that of trickle-bed and monolith reactors (operating at 10 bar) and significantly exceeds that of slurry and liquid-filled membrane reactors.

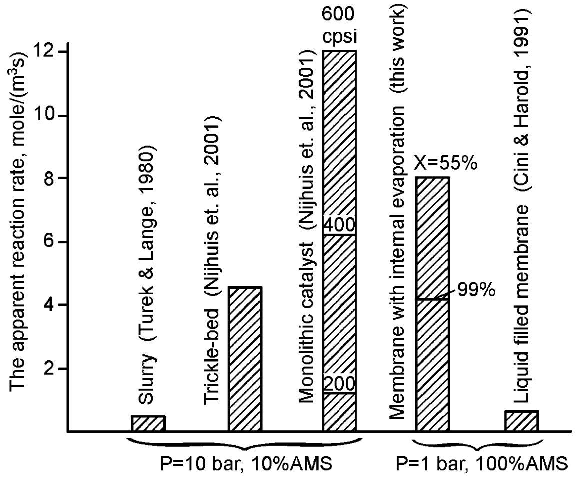

Fig. 6. Comparison of the experimental data on the AMS hydrogenation apparent rate (productivity) per a unit reactor volume for different laboratory reactors.

## 4. Conclusions

A new concept reactor for hydrocarbon hydrogenation in the reactive evaporation mode was preliminary tested and has shown much promise. It safely and efficiently operates in the reaction of hydrogenation of undiluted AMS at normal pressure. Besides, there is no problem of separation of liquid hydrocarbon mixtures, if high conversion is reached within a membrane. The concept of this reactor is similar to that of the microchemical reactor [14]. For instance, the compact reactor design permits an easy scale down if a continuous operation and a low product output are required. In addition, the operation and control of this multiphase reactor are easy. However, a further research is needed to establish its shortcomings and advantages.

## Acknowledgements

This research was financially supported by Copernicus grant ICAS2-1999-10040.

## References

[1] L.B. Datchevich, D.A. Mukhortov, Patent RU 2083540 (1997).
[2] M. Vaarkamp, W. Dijkstra, B.H. Reesink, Catal. Today 69 (2001) 131.
[3] V. Hatziantoniou, B. Andersson, Ind. Eng. Chem. Fundam. 21 (1982) 451.
[4] B. Andersson, S. Irandoust, A. Cybulski, in: A. Cybulski, J.A. Moulijn (Eds.), Marcel Dekker, New York, 1998.
[5] T.A. Nijhuis, M.T. Kreutzer, A.C.T. Romijn, F. Kapteijn, J.A. Moulijn, Chem. Eng. Sci. 56 (2001) 823.
[6] R. de Vos, V. Hatziantoniou, N.H. Shoon, Chem. Eng. Sci. 37 (1982) 1719.
[7] P. Cini, M.P. Harold, Am. Inst. Chem. Eng. J. 37 (1991) 997.
[8] J. Peureux, M. Torres, H. Mozzanega, A. Giroir-Fendler, J.-A. Dalmon, Catal. Today 25 (1995) 409.
[9] M.P. Harold, P.C. Watson, Chem. Eng. Sci. 48 (1993) 981.
[10] P.C. Watson, M.P. Harold, Am. Inst. Chem. Eng. J. 40 (1994) 97.
[11] A. Kulikov, N. Kuzin, A. Shigarov, V. Kirillov, A. Kronberg, K.R. Westerterp, Catal. Today 66 (2001) 255.
[12] A. Shigarov, A. Kulikov, N. Kuzin, V. Kirillov, Chem. Eng. J. 91 (2–3) (2003) 205.
[13] F. Turec, R. Lange, Chem. Eng. Sci. 36 (1980) 569.
[14] D. Honicke, in: G.F. Froment, K.C. Waugh (Eds.), Reaction Kinetics and the Development of Catalytic Processes, Elsevier, Amsterdam, 1999.